2018 European Control Conference (ECC)
June 12-15, 2018. Limassol, Cyprus

Satellite Attitude Fault Tolerant Control with Aerodynamic Disturbance Decoupling

P. Baldi, P. Castaldi, N. Mimmo[1] and S. Simani[2]

Abstract— **This paper presents an Attitude Active Fault Tolerant Control for satellite. The proposed fault tolerant controller is constituted by two main parts: a nominal controller, designed assuming that the system is healthy, and a fault diagnosis module which is in charge of detecting, isolating and estimating the fault affecting the system. The fault diagnosis module is designed by using the NonLinear Geometric Approach which allows for the design of detection residuals and estimation filter decoupled from the aerodynamic disturbance which represents the main uncertainty in low Earth orbits. The simulation results show the benefits, in terms of attitude tracking accuracy, arising when adopting the proposed method.**

I. INTRODUCTION

The increasing operational requirements for on-board autonomy in satellite control systems require structural methods supporting the design of complete and reliable Fault Detection and Diagnosis (FDD) and Fault Tolerant Control (FTC) systems: FDD scheme provide fault detection, isolation and estimation which can be exploited for health monitoring and reconfiguration of the control system [1], [2]. while FTC schemes exploit the faulty, but still working, actuators and sensors required in order to fulfill the mission goals [3]. This motivates the development of control systems that ensure stability, reliability, and required performance even when components fail. In general, FTC methods are classified into two types, i.e. Passive Fault Tolerant Control (PFTC), and Active Fault Tolerant Control (AFTC) [4]. In contrast to PFTCs, which are fixed structure controllers, AFTC systems actively react to faults by reconfiguring the control actionsand heavily rely on realtime Fault Detection and Diagnosis (FDD)FDD modules provide fault estimate which can be used by logic-based switching controller or directly fed–back into the control system. Excellent overviews have been provided for both FDD [5], [6] and FTC [7], and significant research has been done in last decades. Among the proposed approaches, it is worth citing adaptive control, sliding-mode, Lyapunov-based and genetic algorithm approaches (see [3] and citations therein).

The performance of FTCs based on a direct fault estimation feedback are strictly related to the fault estimate accuracy: the smaller is the minimum detectable fault size the earlier is the control reaction while the more accurate is the fault estimate the less is the control performance decay. For these reasons we propose an FDD method which is robustly able to deal with environment uncertainties which for Low Earth Orbits (LEO) are represented by the aerodynamic disturbance.

In particular, this work the NonLinear Geometric Approach (NLGA) to design an FDD module providing fault estimates decoupled from aerodynamic disturbance.

In this paper, we propose a novel AFTC system dealing with faults affecting both actuators sensors. To the authors' knowledge, this is the first AFTC system dealing with the whole set of input and attitude measurement-related faults. This is a significant extension of previous works of the same authors dealing with FDD [9], with new closed-loop stability and fault estimate convergence problems. The NLGA-FDD module provides fault estimates to a standard attitude controller based on a Proportional-Derivative structure suitably modified to directly exploit the fault estimation.

Simulation results are given in case of both multiple satellite actuator and sensor faults, validating the ability to deal with faults of different types, provide precise fault detection, isolation and accurate estimation and obtain the desired attitude control performances.

II. MODELS

This paper presents the dynamics of satellite by means of the definition of two reference frames. The orbit reference frame is indicated by $\mathcal{F}_{\mathcal{O}}(O_O, x_O, y_O, z_O)$ where O_O is located at the centre of gravity of the rigid body, x_O is aligned with the orbit speed, z_O points toward the nadir direction and y_O completes a right-hand orthogonal reference frame. The body fixed reference frame is $\mathcal{F}_{\mathcal{B}}(O_B, x_B, y_B, z_B)$ where O_B coincides with the centre of gravity of the satellite, and the axes x_B, y_B, z_B are aligned with the main principal inertial axis. The attitude of the rigid body is described by a rotation matrix R from the orbit frame $\mathcal{F}_{\mathcal{O}}$ to the body frame $\mathcal{F}_{\mathcal{B}}$. The matrix $R \in SO3$ and is such that $RR^T = I$. The skew matrix is indicated by $S(\cdot) \in \mathbb{R}^{3\times3}$. The angular speed, expressed in $\mathcal{F}_{\mathcal{B}}$ is here indicated with $w \in \mathbb{R}^3$ and the matrix of inertia is denoted by $J \in \mathbb{R}^{3\times3}$ with $J = \text{diag}([J_x, J_y, J_z])$ where $J_x, J_y, J_z \in \mathbb{R}_{>0}$.

A. Satellite

The attitude dynamics of satellite equipped with momentum/reaction wheels, though as a rigid body, is modelled as

[1]The authors are with Department of Electrical, Electronic and Information Engineering "Guglielmo Marconi", University of Bologna, Bologna, Italy {pietro.baldi2; paolo.castaldi;nicola.mimmo2}@unibo.it

[2]Department of Engineering, University of Ferrara, Via Saragat 1, 44122 Ferrara, Italy; silvio.simani@unife.it

follows:

$$\begin{aligned} \dot{R} &= S(w)R \\ J\dot{w} &= -w \times Jw + \frac{3\mu}{r^3}(v_n \times Jv_n) + \\ &\quad u + F_u(t) + p_d(R)d(t) \end{aligned} \tag{1}$$

where $u \in \mathbb{R}^3$ is the control input and the term $d \in \mathbb{R}^{\ell_d}$ indicates the external disturbances such as the aerodynamic force whereas the term $p(R) : \mathbb{R}^{\ell_d} \to \mathbb{R}^3$ is the disturbance input vector field. The term μ indicates the gravitational constant and r represents the orbit radius whereas v_n is the unit vector indicating the nadir direction, expressed in $\mathcal{F}_\mathcal{B}$. Finally, the vector $F_u \in \mathbb{R}^3$ represents the equivalent actuator fault mapped on the satellite dynamics, see Section II-D for details.

B. Sensors

The minimal set of sensors needed to stabilize the attitude of rigid bodies is constituted by three measurements, *i.e.* two non-collinear direction vectors plus the angular speed, [10]. Unfortunately, in case of faults affecting the whole output vector the isolation of faults affecting the direction vector measurements is structurally possible only if there is an hardware redundancy, see [9]. Based on this result, this paper assumes that the rigid body is equipped with the following sensor set:

$$\begin{aligned} y_{i,j} &= Rv_i + F_{y_{i,j}} + \nu_{i,j} \quad i,j \in \{1,2\} \\ y_{3,1} &= w + F_{y_{3,1}} + \nu_{3,1} \end{aligned} \tag{2}$$

where $y_{i,j} \in \mathbb{R}^3$ for all $i = 1, \ldots, 3$. The terms $F_{y_{i,j}} \in \mathbb{R}^3$, with $i = 1, \ldots, 3$ represent the faults affecting the output. Moreover $\nu_{i,j}$ indicates the noise associated to the (i,j)-th sensor. Moreover, the unit vectors v_1, $v_2 \in \mathbb{R}^3$ are defined in $\mathcal{F}_\mathcal{O}$ and are not collinear. Finally, the output $y_{1,2}$ and $y_{2,2}$ represent the attitude sensors hardware redundancy.

C. Aerodynamic Disturbances

Satellites flying close to planets characterized by the presence of atmosphere are subject to external aerodynamic forces which, in turns, generates disturbance torques. Commonly these effects are modelled as follows:

$$\begin{aligned} p_d(R) &= r_{\text{a.p.c.}} \times Rv_{v_I} \\ d(t) &= \tfrac{1}{2}\rho(t)V^2 S C_D \end{aligned} \tag{3}$$

where the unit vector v_{v_I} indicates the versor of the orbit speed, expressed in $\mathcal{F}_\mathcal{O}$, the vector $r_{\text{a.p.c.}}$ indicated the distance from the center of gravity to the aerodynamic pressure center, expressed in $\mathcal{F}_\mathcal{B}$, the $d(t)$ represents the aerodynamic force, usually modelled as product of the air density ρ times the square of the orbit speed V times the drag coefficient C_D. In this scenario the aerodynamic force $d(t)$ is unknown because both the air density ρ and the drag coefficient C_D are unknown.

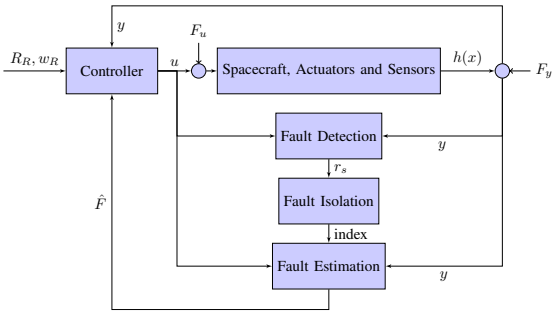

Fig. 1: Representation of the Active Fault Tolerant Control System.

D. Faults

The system is affected by faults on the sensors set and on actuators for a total number of faults equal to $n_F = 8$. The faults influencing the sensors are modelled as variations of the characteristic curve plus a bias, i.e.

$$F_{y_i}(t) = b_{y_i}(t) + (k_{y_i}(t) - 1)h_i(x) \tag{4}$$

where $k_{y_i}(t) : \mathbb{R}_{>0} \to \mathbb{R}_{\geq 0}$ and $b_{y_i}(t) : \mathbb{R}_{\geq 0} \to \mathbb{R}$ represent the fault parameters. On the other hand, satellites are usually equipped with $n_a \geq 3$ actuators (torque generators) which, for the case of momentum/reaction wheels, can be modelled as follows:

$$\begin{aligned} J_a\dot{w}_a &= M_a + F_a(t) - bw_a \\ F_a(t) &= -\beta_0(t)\text{sign}(w_a) - \beta_1(t)w_a \end{aligned} \tag{5}$$

where $w_a \in \mathbb{R}^{n_a}$ represents the actuators speed, J_a indicates the flywheels inertia, b is the friction coefficient and M_a is the actuator control torque. The term $F_a(t)$ indicates the fault vector which is modelled as an external torque independent from the wheel speed, modulated by $\beta_0(t) : \mathbb{R}_{\geq 0} \to \mathbb{R}_{>0}$, plus a time varying term proportional to the actual flywheel speed, modulated by $\beta_1(t) : \mathbb{R}_{\geq 0} \to \mathbb{R}_{>0}$. The actuator control torque is related to the nominal satellite control torque u by means of the following relation, [11]:

$$M_a = bw_a + \phi(\tilde{w}_a) - A^\star\left(w \times (AJ_a w_a^R) + u\right) \tag{6}$$

where $\tilde{w}_a = w_a^R - w_a$. The matrix $A : \mathbb{R}^{n_a} \to \mathbb{R}^3$ is the map which combines the effects of the actuators on the satellite and, in particular, the i-th column represents the unit vector indicating the spin axis of the i-th actuator, expressed in F_B. The term $A^\star : \mathbb{R}^3 \to \mathbb{R}^{n_a}$ denotes an optimization map from the required satellite torques u to the effective torque on the n_a actuators and $\phi(\cdot)$ represents any stabilizing controller which make w_a tracking the reference $w_a^R(t)$. The reference flywheel spin rate $w_a^R(t)$ is generated by the following internal model

$$J_a\dot{w}_a^R = -A^\star\left(w \times (AJ_a w_a^R) + u\right) \tag{7}$$

Finally the equivalent fault $F_u(t)$ is obtained by comparing the actual satellite input $u_{\text{act}} = -AJ_a\dot{w}_a - w \times AJ_a w_a$ with the nominal u leading to:

$$\begin{aligned} F_u(t) &= w \times AJ_a\tilde{w}_a - A\phi(\tilde{w}_a) - AF_a(t) = \\ &= AJ_a\dot{\tilde{w}}_a + w \times AJ_a\tilde{w}_a \end{aligned} \tag{8}$$

It is important to remark that, even in presence of a controller $\phi(\cdot)$ which asymptotically makes null $\tilde{w}_a$ despite the presence of fault F_a, the $F_u(t)$ remains detectable during the transient phases (*i.e.* even in the hypothesis of a full knowledge of the internal model of the fault $F_a(t)$, the discontinuity introduced by the fault occurrence induces an inevitable transient phase).

E. Overall model

The design of the attitude AFTC is based on the following mathematical representation of the satellite dynamics (1)-(2):

$$\begin{aligned} \dot{x} &= g_0(x) + \sum_{i=1}^{3} g_i(x)u_i + \ell F_u(t) + p(x)d(t) \\ y &= h(x) + F_y(t) \end{aligned} \tag{9}$$

where $x = [R,\, w]^T$ is the state space vector, $y = [y_{1,1}, \ldots, y_{3,1}]^T$ indicates the output, ℓ and p are the actuator fault and aerodynamic disturbance input vector fields respectively. The vector fields g_i with $i = 0, \ldots, 3$, ℓ and $p(x)$ and the smooth map $h(x)$ are defined as follows:

$$\begin{aligned} g_0 &= \begin{bmatrix} S(w)R \\ J^{-1}\left(-w \times Jw + \dfrac{3\mu}{r^3}(v_n \times Jv_n)\right) \end{bmatrix} \\ \ell &= [g_1,\, g_2,\, g_3] = \begin{bmatrix} 0_{3\times 3} \\ J^{-1} \end{bmatrix} \\ p(x) &= \begin{bmatrix} 0_{3\times 1} \\ J^{-1}\left(r_{\text{a.p.c.}} \times Rv_{v_I}\right) \end{bmatrix} \\ h(x) &= [Rv_1, Rv_1, Rv_2, Rv_2, w]^T \end{aligned} \tag{10}$$

III. ATTITUDE ACTIVE FAULT TOLERANT CONTROL

A. Adaptive Controller

Given the reference attitude generated by

$$\dot{R}_R = S(w_R(t))R_R \tag{11}$$

with $w_R(t)$ known, the goal of the control is to steer the actual attitude $R(t)$ to the reference $R_R(t)$. The rotation matrix R_c is calculated by means of the TRIAD procedure detailed in [12] and using the outputs $y_{1,1}$ and $y_{2,1}$ (which are affected by faults). The attitude error between the reference rotation matrix $R_R(t)$ and the satellite calculated rotation matrix $R_c(F_y)$, defined in $SO3$, is described by the rotation matrix $\tilde{R}(F_y) = R_R(t)R_c^T(F_y)$. It is defined with $q(t, F_y)$ the quaternion associated to $\tilde{R}(t, F_y)$ and denote with $\epsilon(t, F_y) \in \mathbb{R}^3$ its complex vectorial part which is clearly affected by the fault F_y. Given the system in (9) the control goal is the asymptotic tracking $\epsilon(t)$ to zero:

$$\lim_{t\to\infty} \epsilon(t, \cdot) = 0 \tag{12}$$

despite the presence of faults. The attitude control law is represented by the output of a PD controller (output feedback) usually implemented in satellites, [13]:

$$\begin{aligned} u &= -k_p\epsilon(F_y) + y_1 \times Jy_1 \\ &\quad -k_d(y_1 - \tilde{R}(F_y)w_R) = \\ &= -k_p\epsilon(F_y) + (w + F_{y_1}) \times J(w + F_{y_1}) \\ &\quad -k_d(w + F_{y_1} - \tilde{R}(F_y)w_R) \end{aligned} \tag{13}$$

where $k_p,\, k_d > 0$ are the PD control parameters to be designed whereas the term $w \times Jw$ compensates the satellite gyroscopic effects. As stated in [13] this class of controllers assures asymptotic stability in absence of faults. The presence of faults F_y and F_u requires a modification of the nominal controller (13) to keep the stabilizing properties of the fault free controller. In particular this paper proposes to subtract a direct estimation of the faults into the control algorithm as follows:

$$\begin{aligned} u &= -k_p\epsilon(F_y - \hat{F}_y) - \hat{F}_u + \\ &\quad +(w + F_{y_1} - \hat{F}_{y_1}) \times J(w + F_{y_1} - \hat{F}_{y_1}) + \\ &\quad -k_d(w + F_{y_1} - \hat{F}_{y_1} - \tilde{R}(F_y - \hat{F}_y)w_R) \end{aligned} \tag{14}$$

where $\hat{F}_y$ and $\hat{F}_u$ indicates the estimation of the faults affecting the output and the input respectively. Figure 1 depicts the scheme of the proposed AFTC.

B. Fault Detection and Diagnosis Module

In this paper, the estimation of faults affecting both the input and output is selectively performed only after a fault detection and isolation process. To detect and isolate faults affecting both the input and output we first introduce a dynamic extension of the output as follows:

$$\begin{aligned} \dot{z} &= h(x) + F_y(t) \\ \mu &= z \end{aligned} \tag{15}$$

With a small abuse of notation this paper lists the elements of μ as $\mu_{1,1}$, $\mu_{1,2}$, …, $\mu_{3,1}$ to keep trace of the output nomenclature. The overall model, union of (9) and (15), becomes:

$$\begin{aligned} \dot{\chi} &= \xi_0(\chi) + \sum_{i=1}^{3} \xi_i(\chi)u_i + \ell_F F(t) + \ell_d(\chi)d(t) \\ \mu &= \eta(\chi) \end{aligned} \tag{16}$$

where $\chi = [x,\, z]^T$, $F = [F_u,\, F_y]^T$, $\mu = z$ and

$$\begin{aligned} \xi_0(\chi) &= \begin{bmatrix} g_0(x) \\ h(x) \end{bmatrix} \quad \xi_i(\chi) = \begin{bmatrix} g_i(x) \\ 0 \end{bmatrix} \\ \ell_F &= \begin{bmatrix} \ell & 0 \\ 0 & I \end{bmatrix} \quad \ell_d = \begin{bmatrix} p(x) \\ 0 \end{bmatrix} \end{aligned} \tag{17}$$

Let us define the fault set

$$f = \{F_{u_1}, \ldots, F_{u_{n_a}}, F_{y_{1,1}}, \ldots, F_{y_{3,1}}\}$$

and the selected fault subset as $f_s \subseteq f$. Furthermore, let us define the generalized disturbance d_s associated to f_s as the set $d_s := \{(f \setminus f_s) \cup d\}$. The fault detection and isolation is performed by means of the design of a bank of residuals each one sensitive to a different subset f_s. In particular, there exist a class $\mathcal{K}_\infty$ function $\gamma(\cdot) : [0, \infty) \to [0, \infty)$ and a class

$\mathcal{KL}$ function $\beta(\cdot,\cdot) : [0,\infty) \times [0,\infty) \to [0,\infty)$ such that the behaviour of each residual $r(t)$ can be described by:

$$|r(t)| \leq \beta(|r(0)|, t) + \gamma(||f_s||_\infty) \quad \forall\, t \geq 0 \tag{18}$$

Moreover, let us denote with n_R the number of residuals and with $\Omega_s \subseteq \{1, \ldots, n_R\}$ the set of residuals affected by the subset f_s. Then, the sufficient condition for solving the FDI problem, i.e. to detect and isolate each fault subset f_s, is to design n_R residuals such that each fault in f_s affect a different and non empty subset Ω_s of residuals.

This paper approaches to the design of these n_R residuals by means of the NonLinear Geometric Approach (NLGA) which, defined the f_s, allows for the definition of couples of (local) diffeomorphisms (one in the state space, $\Phi(\chi)$, and the other one in the output space, $\Psi(\mu)$) generating new systems in which the associated d_s is not present, see [8] and [14]:

$$\begin{cases} \Phi(\chi) &= \begin{pmatrix} \bar{\chi}_1 & \bar{\chi}_2 & \bar{\chi}_3 \end{pmatrix}^T \\ \Psi(\mu) &= \begin{pmatrix} \bar{\mu}_1 & \bar{\mu}_2 \end{pmatrix}^T \end{cases} \tag{19}$$

If the coordinate changes in (19) can be found, the system (16), in the new reference frame, can be decomposed into three subsystems where the first one (the so–called $\bar{\chi}_1$–subsystem) is always de–coupled from the disturbance vector d_s and affected by the generalized faults set f_s. For the considered case the $\bar{\chi}_1$–subsystem assumes the following structure:

$$\begin{aligned} \dot{\bar{\chi}}_1 &= n_1(\bar{\chi}_1, \bar{\mu}_2) + g_1(\bar{\chi}_1, \bar{\mu}_2)\, u + \ell_{s_1}(\bar{\chi}_1, \bar{\mu}_2)\, f_s \\ \bar{\mu}_1 &= \eta_1(\bar{\chi}_1) \end{aligned} \tag{20}$$

Even if the state $\bar{\chi}_3$ is not available for direct measurements, the detection of f_s is always guaranteed by observing that, since $\ell_{s_1}(\bar{\chi})$ is not identically zero, the presence of f_s can be always find out by designing a filter for the detection of $\ell_{s_1} f_s$. Thanks to the double application of the NLGA on the redundant set of attitude sensors, it is possible to define eight detection systems. In particular given $j, k \in \{1, 2\}$ the complementary indexes are defined as $\bar{j} = \{1, 2\} \setminus j$ and $\bar{k} = \{1, 2\} \setminus k$. Furthermore the term e_q, where $q = 1, 2, 3$, indicates the unit vector along the first, second and third axis of $\mathcal{F}_\mathcal{B}$, we have:

1st to 4th detection systems

$$\begin{aligned} f_s &= \{F_{y_{1,j}}, F_{y_{2,k}}, F_{y_{3,1}}\} \\ d_s &= \{F_{y_{1,\bar{j}}}, F_{y_{2,\bar{k}}}, F_{u_1}, F_{u_2}, F_{u_3}, d\} \\ \bar{\chi}_1 &= R \\ \dot{\bar{\mu}}_1 &= [y_{1,j_1}, y_{2,j_2}]^T \end{aligned} \tag{21}$$

5th to 8th detection systems

$$\begin{aligned} f_s &= \{F_{y_{1,j}}, F_{y_{2,k}}, F_{y_{3,1}}, F_{u_2}, F_{u_3}\} \\ d_s &= \{F_{y_{1,\bar{j}}}, F_{y_{2,\bar{k}}}, F_{u_1}, d\} \\ \dot{\bar{\chi}}_1 &= e_1^T \left(\left((Rv_v) r_{\text{a.c.p.}}^T - r_{\text{a.c.p.}}(Rv_v)^T \right) w \right) \\ \dot{\bar{\mu}}_1 &= e_1^T \left(\left((R_{c,i} v_v) r_{\text{a.c.p.}}^T - r_{\text{a.c.p.}}(R_{c,i} v_v)^T \right) y_{3,1} \right) \end{aligned} \tag{22}$$

TABLE I: Residual Matrix, RM

	$F_{y_{1,1}}$	$F_{y_{2,1}}$	$F_{y_{1,2}}$	$F_{y_{2,2}}$	$F_{y_{3,1}}$	F_{u_1}	F_{u_2}	F_{u_3}
r_1	X	X	0	0	X	0	0	0
r_2	X	0	0	X	X	0	0	0
r_3	0	X	X	0	X	0	0	0
r_4	0	0	X	X	X	0	0	0
r_5	X	X	0	0	X	0	X	X
r_6	X	0	0	X	X	0	X	X
r_7	0	X	X	0	X	0	X	X
r_8	0	0	X	X	X	0	X	X
r_9	X	X	0	0	X	X	0	X
r_{10}	X	0	0	X	X	X	0	X
r_{11}	0	X	X	0	X	X	0	X
r_{12}	0	0	X	X	X	X	0	X
r_{13}	X	X	0	0	X	X	X	0
r_{14}	X	0	0	X	X	X	X	0
r_{15}	0	X	X	0	X	X	X	0
r_{16}	0	0	X	X	X	X	X	0

9th to 12th detection systems

$$\begin{aligned} f_s &= \{F_{y_{1,j}}, F_{y_{2,k}}, F_{y_{3,1}}, F_{u_1}, F_{u_3}\} \\ d_s &= \{F_{y_{1,\bar{j}}}, F_{y_{2,\bar{k}}}, F_{u_2}, d\} \\ \dot{\bar{\chi}}_1 &= e_2^T \left(\left((Rv_v) r_{\text{a.c.p.}}^T - r_{\text{a.c.p.}}(Rv_v)^T \right) w \right) \\ \dot{\bar{\mu}}_1 &= e_2^T \left(\left((R_{c,i} v_v) r_{\text{a.c.p.}}^T - r_{\text{a.c.p.}}(R_{c,i} v_v)^T \right) y_{3,1} \right) \end{aligned} \tag{23}$$

13th to 16th detection systems

$$\begin{aligned} f_s &= \{F_{y_{1,j}}, F_{y_{2,k}}, F_{y_{3,1}}, F_{u_1}, F_{u_2}\} \\ d_s &= \{F_{y_{1,\bar{j}}}, F_{y_{2,\bar{k}}}, F_{u_3}, d\} \\ \dot{\bar{\chi}}_1 &= e_3^T \left(\left((Rv_v) r_{\text{a.c.p.}}^T - r_{\text{a.c.p.}}(Rv_v)^T \right) w \right) \\ \dot{\bar{\mu}}_1 &= e_3^T \left(\left((R_{c,i} v_v) r_{\text{a.c.p.}}^T - r_{\text{a.c.p.}}(R_{c,i} v_v)^T \right) y_{3,1} \right) \end{aligned} \tag{24}$$

1) Detection residuals and residual matrix: Given the detection systems of equations (21)-(24), the analogical detection residuals are obtained by means of filters as follows:

$$\begin{aligned} \dot{\hat{\bar{\chi}}}_1 &= n_1(\hat{\bar{\chi}}_1, H_2\mu) + g_1(\hat{\bar{\chi}}_1, H_2\mu)\, u + \alpha_s \text{sign}(\xi_s) \\ \xi_s &= \Psi_1(\mu) - \hat{\bar{\chi}}_1 \end{aligned} \tag{25}$$

where the constant α_s is a positive diagonal matrix properly designed and sign$(\cdot)$ represents a vector which elements are the sign function of each element of ξ_s. The residual r_s is defined as follows:

$$r_s = \{(\alpha_s \text{sign}(\xi_s))\}_{\text{eq}} \tag{26}$$

where $\{(\cdot)\}_{\text{eq}}$ indicates a low passed (equivalent) version of $(\cdot)$. The binary version of r_s is obtained by the following logic:

$$r_s^d \;=\; \begin{cases} 0 & \sqrt{r_s^T W_s r_s} \leq r_s^{\text{th}} \\ 1 & \sqrt{r_s^T W_s r_s} > r_s^{\text{th}} \end{cases} \tag{27}$$

where $r_s^{\text{th}} := \sup_\nu \sqrt{r_s^T W_s r_s}$ with $F_y = 0$, $F_u = 0$ and where ν represents the vector of sensor noises.

The $n_R = 16$ residuals are collected into the so called residual matrix RM which is a $n_R \times n_F$ matrix whose (i, j) element is a binary 0 if the i-th residual is not affecting by the j-th fault. The residual matrix is completed by elements equal to X which are equal to 1 if the corresponding $r_i^d = 1$. As can be see in Table I, the isolation of faults affecting the output $\{F_{y_{1,1}}, F_{y_{2,1}}\}$ and $\{F_{y_{1,2}}, F_{y_{2,2}}\}$ is not possible without hardware redundancy.

2) Estimation Filters: The particular structure of the detection residuals make them suitable also for the estimation of faults. In detail, assuming that

$$\begin{aligned}\alpha_{s_i} \quad > \quad & \big|\big| n_{1_i}(\bar{\chi}_1, H_2\mu) - n_{1_i}(\hat{\bar{\chi}}_1, H_2\mu) + \\ & + (g_{1_i}(\bar{\chi}_1, H_2\mu) - g_{1_i}(\hat{\bar{\chi}}_1, H_2\mu))\, u + \\ & + \ell_{s_{1_i}}(\bar{\chi}_1, \bar{\mu}_2, \bar{\chi}_3)\, f_s \big|\big|_\infty \end{aligned} \tag{28}$$

for each i-th element of $\bar{\chi}_1$, then the stability of the detection residual is guaranteed and the following hold:

$$\lim_{t\to\infty} \{(\bar{\chi}_1 - \hat{\bar{\chi}}_1)\}_{\text{eq}} = 0 \tag{29}$$

As consequence, asymptotically the equivalent value of the residual is directly proportional to the fault f_s which contains only one elements, *i.e,* the isolated fault:

$$\lim_{t\to\infty} \{\alpha_s \text{sign}(\xi_s)\}_{\text{eq}} = \ell_{s_1}(\bar{\chi}_1, \bar{\mu}_2, \bar{\chi}_3)\, f_s \tag{30}$$

Finally, since by definition $\ell_{s_1}(\bar{\chi}_1, \bar{\mu}_2, \bar{\chi}_3) \neq 0$ for all $t \geq 0$, the fault estimation is accomplished by:

$$\hat{f}_s = \ell_{s_1}(\bar{\chi}_1, \bar{\mu}_2, \bar{\chi}_3)^{-1} \{\alpha_{1_s} \text{sign}(\xi_s)\}_{\text{eq}} \tag{31}$$

which asymptotically converges to the actual fault value

$$\lim_{t\to\infty} \hat{f}_s = f_s \tag{32}$$

IV. EXPERIMENTAL RESULTS

The satellite is modelled as a rigid body with inertia matrix given by $J = \text{diag}([330,\ 150,\ 140])$ kg·m^2. The aerodynamic centre of pressure is located at $r_{\text{a.c.p.}} = [0.10,\ 0.15,\ -0.25]$ meters expressed in $\mathcal{F}_\mathcal{B}$ whereas the drag coefficient has been taken as $C_D = 2.2$, the air density equal to $\rho = 9.158 \cdot 10^{-12}$ kg/m^3 and the orbit speed $V = 8187.63$ m/s. The gravitational disturbance is characterized by a gravitational constant $\mu = 39.86004418 \cdot 10^{13}$ m^3/s^2 and the orbit radius has been fixed to $r = 6728.140$ Km (350 km above the sea level). The initial nominal actuators flywheel spin rate is 3000 rpm with a nominal value of $b = 5.16 \cdot 10^{-6}$ Nms. Furthermore, the actuator input matrix considered in these tests is $A = I_{3\times 3}$. Finally, at time $t = 0$ the satellite is standing aligned with the orbit reference frame, *i.e.* $\mathcal{F}_\mathcal{B}(t = 0) \equiv \mathcal{F}_\mathcal{O}(t = 0)$, $w(t = 0) = 0$.

The results presented in this section show the detection and isolation performance, the estimation performance and, finally the trajectory tracking improvements due to the proposed active fault tolerant controller. In detail, Figures 2-5 depicts the behaviour of the residuals in presence of a fault affecting the sensor $y_{1,1}$, $F_{3,1}$, and Figure 6-9 reports the behaviour of the residuals when in presence of a fault on the first input channel, F_{a_1}. Figures from 2 to 9 reports, with dashed lines, the values of the thresholds r_d^{th}. As can be seen the residuals match the configurations listed in Table I for the corresponding faults thus leading to a correct isolation even in presence of the aerodynamic disturbance. The fault estimation performances can be appreciated in Figures 10-11 where it is possible to identify the detection and isolation time need to correctly identify the residuals configurations in Table I. Finally, Figures from 12 to 13 clearly show, even in presence of a manoeuvre, the tracking accuracy improvement which can be reached by adopting the proposed active fault tolerant control scheme. In these pictures the dashed lines represent the trajectory in presence of faults whereas the continuous lines indicate the reference trajectory in absence of fault. Furthermore this paper presents also the results of a Monte Carlo test campaign (10000 runs) in which the faults have been randomly generated, among the eight possible faults, with a probability space Γ, with uniform probability density, into the following measurable spaces

TABLE II: Monte Carlo Simulation Results

Fault	MDR	WIS	RIS	EA $\cdot 10^{-3}$	TAWO $\cdot 10^{5}$	TAW $\cdot 10^{4}$
$F_{y_{i,j}}$	0	0	100	0.0458	2.9759	1.1250
$F_{y_{3,1}}$	0	0	100	474	1.7207	5.3968
F_{u_1}	0.8	0	99.2	0.066	0.3494	1.5823
F_{u_2}	3.5	0	96.5	0.193	0.3070	1.0231
F_{u_3}	1.7	0	98.3	0.070	0.3197	1.2017

$$\begin{gathered} b_{y_{1,1}}, b_{y_{1,2}}, b_{y_{2,1}}, b_{y_{2,2}} : \Gamma \to E_{b_{1-2}} \\ k_{y_{1,1}}, k_{y_{1,2}}, k_{y_{2,1}}, k_{y_{2,2}} : \Gamma \to E_{k_{1-2}} \\ b_{y_{3,1}} : \Gamma \to E_{b_3} \quad k_{y_{3,1}} : \Gamma \to E_{k_3} \\ \beta_0 : \Gamma \to E_{\beta_0} \quad \beta_1 : \Gamma \to E_{\beta_1} \end{gathered} \tag{33}$$

with $E_{b_{1-2}} = [-1,\ 1] \cdot 0.09$, $E_{k_{1-2}} = [0.90,\ 1.10]$, $E_{b_3} = [-1,\ 1] \cdot 2.8 \cdot 10^{-5}$ arcsec/s, $E_{k_3} = [0.90,\ 1.10]$, $E_{\beta_0} = [0,\ 1] \cdot 0.02$ Nm and $E_{\beta_1} = [0,\ 1] \cdot 10b$. The results of the Monte Carlo campaign are collected in table II where the following indexes have been identified:

- Missed Detection Rate (MDR): percentage of simulation in which the fault is not detected;
- Wrong Isolation Rate (WIR): percentage of simulations for which the isolation process gives wrong results;
- Right Isolation Rate (RIS): percentage of cases in which the isolation logic correctly identify the occurred fault;
- Estimation Accuracy (EA): standard deviation of the (asymptotic) fault estimation errors, with the proper physical dimension (arcsec/s for the gyroscopes and Nm for the actuators);
- Tracking Accuracy WithOut the AFTC (TAWO): standard deviation of the tracking error expressed in arcsec, without the proposed AFTC, with respect to the nominal trajectory in absence of faults;
- Tracking Accuracy With the AFTC (TAW): standard deviation of the tracking error expressed in arcsec, with the proposed AFTC, with respect to the nominal trajectory in absence of faults.

Table II shows that, thanks to the hardware redundancy the possibility of a missed detection in case of faults affecting the attitude sensors is practically eliminated whereas, due to the different satellite inertia, the different sensitivity of the residuals to the faults affecting the actuators implies different isolability capabilities (with respect to the same input fault). A second important insight that can be obtained by observing table II is that the proposed AFTC reduces, by a factor 2, the trajectory tracking errors.

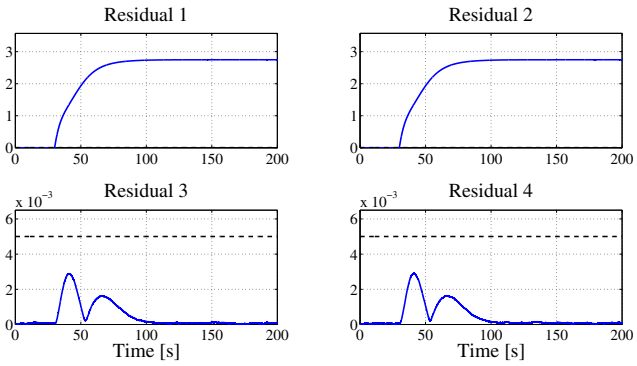

Fig. 2: Residuals from 1st to 4th with fault $F_{y_{1,1}} = [0.10,\ 0.12,\ -0.07]^T$

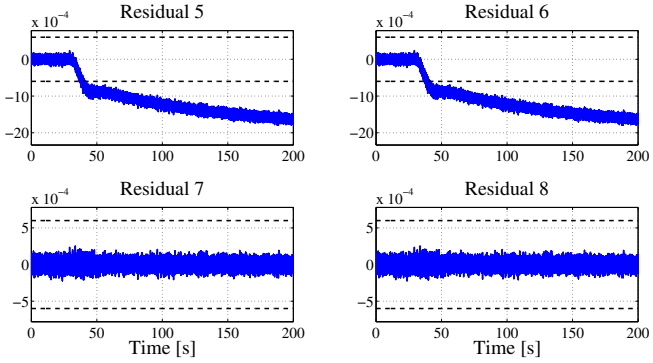

Fig. 3: Residuals from 5th to 8th with fault $F_{y_{1,1}} = [0.10,\ 0.12,\ -0.07]^T$

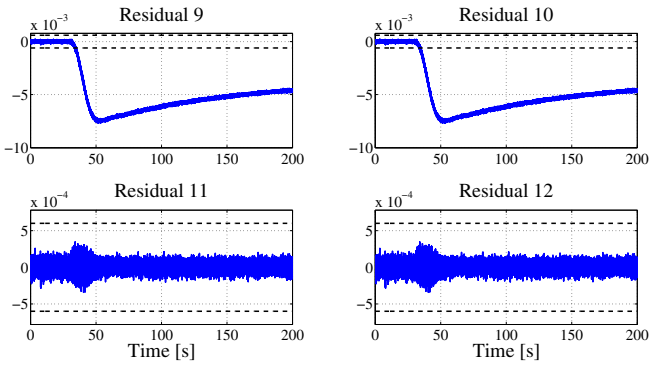

Fig. 4: Residuals from 9th to 12th with fault $F_{y_{1,1}} = [0.10,\ 0.12,\ -0.07]^T$

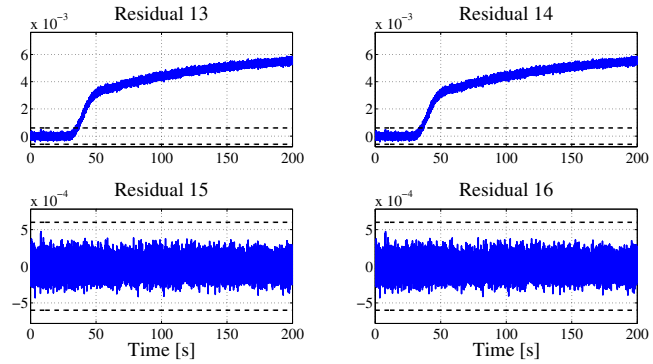

Fig. 5: Residuals from 13th to 16th with fault $F_{y_{1,1}} = [0.10,\ 0.12,\ -0.07]^T$

V. Conclusions

This work presented an attitude active fault tolerant control which exploits the nonlinear geometric approach for the fault detection, isolation and estimation process. Thanks to this approach both the detection residuals and the fault estimation are analytically decoupled from the aerodynamic disturbance which represents the main unknown input in a low Earth orbit satellite. The simulation results, also in terms of tracking accuracy, confirm the benefits arising from the adoption of the proposed solution. Further developments will analytically investigate the stability of the proposed attitude active fault tolerant control.

References

[1] X. Olive, "Fdi (r) for satellite at thales alenia space how to deal with high availability and robustness in space domain?" in *Control and Fault-Tolerant Systems (SysTol), 2010 Conference on*. IEEE, 2010, pp. 837–842.

[2] P. Baldi, P. Castaldi, N. Mimmo, and S. Simani, "A new aerodynamic decoupled frequential fdir methodology for satellite actuator faults," *International Journal of Adaptive Control and Signal Processing*, vol. 28, no. 9, pp. 812–832, 2014.

[3] S. Yin, B. Xiao, S. X. Ding, and D. Zhou, "A review on recent development of spacecraft attitude fault tolerant control system," *IEEE Transactions on Industrial Electronics*, vol. 63, no. 5, pp. 3311–3320, 2016.

[4] M. Blanke, M. Kinnaert, J. Lunze, M. Staroswiecki, and J. Schröder, *Diagnosis and fault-tolerant control*. Springer, 2006, vol. 691.

[5] J. Bokor and Z. Szabó, "Fault detection and isolation in nonlinear systems," *Annual Reviews in Control*, vol. 33, no. 2, pp. 113–123, 2009.

[6] J. Chen and R. J. Patton, *Robust model-based fault diagnosis for dynamic systems*. Springer Science & Business Media, 2012, vol. 3.

[7] Y. Zhang and J. Jiang, "Bibliographical review on reconfigurable fault-tolerant control systems," *Annual reviews in control*, vol. 32, no. 2, pp. 229–252, 2008.

[8] C. De Persis and A. Isidori, "A geometric approach to nonlinear fault detection and isolation," *IEEE transactions on automatic control*, vol. 46, no. 6, pp. 853–865, 2001.

[9] P. Baldi, M. Blanke, P. Castaldi, N. Mimmo, and S. Simani, "Combined geometric and neural network approach to generic fault diagnosis in satellite actuators and sensors," *IFAC-PapersOnLine*, vol. 49, no. 17, pp. 432–437, 2016.

[10] J. R. Wertz, *Spacecraft attitude determination and control*. Springer Science & Business Media, 2012, vol. 73.

[11] B. Wie, *Space vehicle dynamics and control*. Aiaa, 1998.

[12] G. Wahba, "A least squares estimate of satellite attitude," *SIAM review*, vol. 7, no. 3, pp. 409–409, 1965.

[13] J.-Y. Wen and K. Kreutz-Delgado, "The attitude control problem," *IEEE Transactions on Automatic control*, vol. 36, no. 10, pp. 1148–1162, 1991.

[14] M. Bonfè, P. Castaldi, N. Mimmo, and S. Simani, "Active fault tolerant control of nonlinear systems: The cart-pole example," *International Journal of Applied Mathematics and Computer Science*, vol. 21, no. 3, pp. 441–445, 2011.

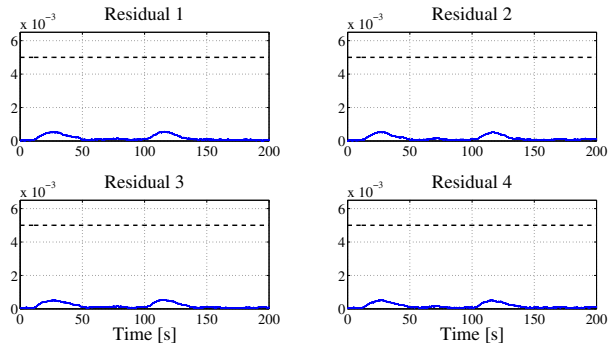

Fig. 6: Residuals from 1st to 4th with fault $F_{a_1} = -10bw_a$ Nm

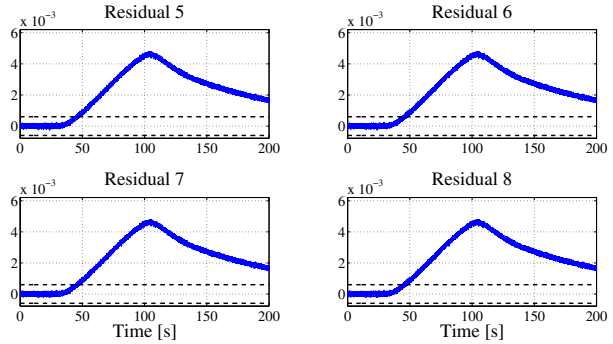

Fig. 7: Residuals from 5th to 8th with fault $F_{a_1} = -10bw_a$ Nm

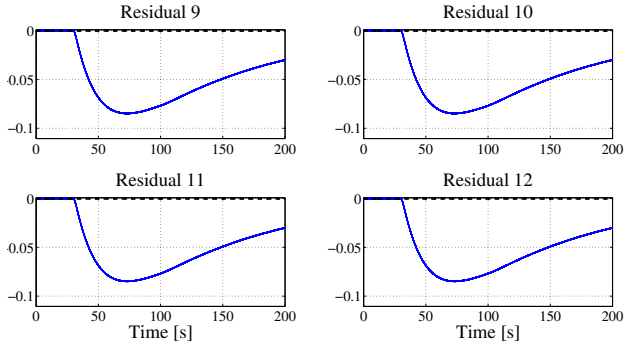

Fig. 8: Residuals from 9th to 12th with fault $F_{a_1} = -10bw_a$ Nm

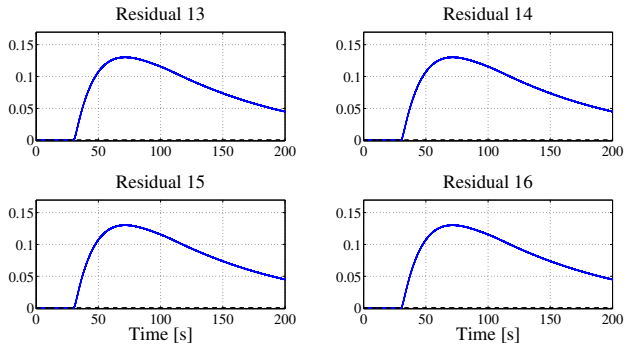

Fig. 9: Residuals from 13th to 16th with fault $F_{a_1} = -10bw_a$ Nm

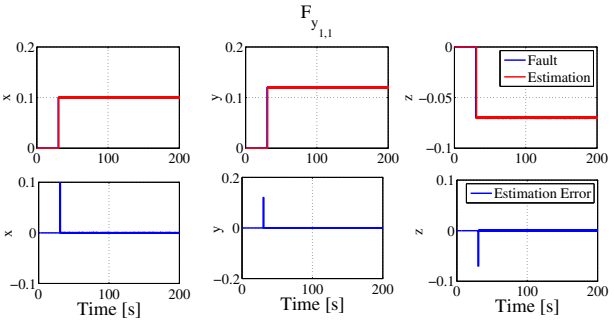

Fig. 10: Estimation of fault $F_{y_{1,1}} = [0.10,\ 0.12,\ -0.07]^T$

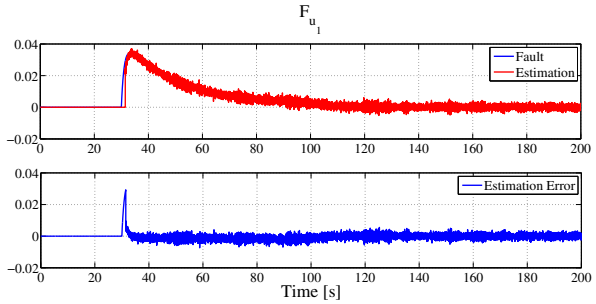

Fig. 11: Estimation of fault F_{u_1}

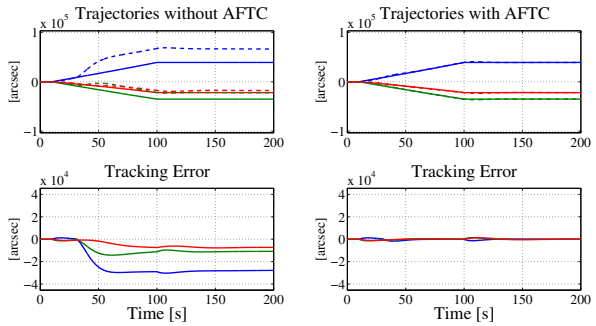

Fig. 12: Trajectories with and without the AFTC in presence of fault $F_{y_{1,1}} = [0.10,\ 0.12,\ -0.07]^T$ appearing at time $t = 30$ s.

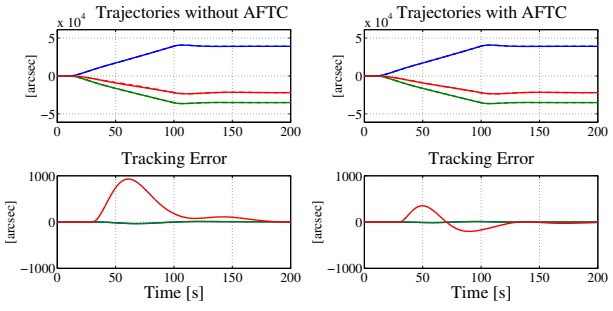

Fig. 13: Trajectories with and without the AFTC in presence of fault $F_{a_1} = -10bw_a$ Nm appearing at time $t = 30$ s.